Eur. Phys. J. C 30, 111–116 (2003)
Digital Object Identifier (DOI) 10.1140/epjc/s2003-01255-8

THE EUROPEAN PHYSICAL JOURNAL C

Strange particle production at RHIC in the dual parton model

A. Capella[1], C.A. Salgado[2], D. Sousa[3]

[1] Laboratoire de Physique Théorique[a], Université de Paris XI, Bâtiment 210, 91405 Orsay Cedex, France
[2] Theory Division, CERN, 1211 Geneva 23, Switzerland
[3] ECT[a], Villa Tambosi, Strada delle Tabarelle 286, 38050 Villazzano, Trento, Italy

Received: 28 April 2003 /
Published online: 11 July 2003 –

Abstract. We compute the mid-rapidity densities of pions, kaons, baryons and antibaryons in Au–Au collisions at $\sqrt{s} = 130\,\mathrm{GeV}$ in the dual parton model supplemented with final state interaction (comovers interaction). The ratios B/n_{part} ($\overline{B}/n_{\mathrm{part}}$) increase between peripheral ($n_{\mathrm{part}} = 18$) and central ($n_{\mathrm{part}} = 350$) collisions by a factor 2.4 (2.0) for the Λ, 4.8 (4.1) for the Ξ and 16.5 (13.5) for the Ω. The ratio K^-/π^- increases by a factor 1.3 in the same centrality range. A comparison with the available data is presented.

1 Introduction

The enhancement of yields of strange baryons and antibaryons per participant nucleon, observed at CERN-SPS [1,2], is one of the main results of the Heavy Ion CERN program. A description of these data has been given in [3] in the framework of the dual parton model (DPM) [4], supplemented with a final state interaction. The net baryon yield is computed in the same framework taking into account the mechanism of baryon stopping, associated with baryon junction transfer in rapidity [5–9]. We use its implementation in [3], which describes the SPS data.

In this work this formalism is extended to RHIC energies. In Sect. 2 we give the DPM formula to compute single particle inclusive production. In the case of baryon production, this formula only gives $B\overline{B}$ pair production. The corresponding formula for net baryon production ($B-\overline{B}$) is given in Sect. 3. In Sect. 4 we introduce final state interaction (comovers interaction). Numerical results are presented in Sect. 5. In Sect. 6 we compare the results at SPS and RHIC energies, discuss their physical interpretation and present our conclusions.

2 The model

In the absence of nuclear shadowing, the rapidity density of a given type of hadron h produced in AA collisions at fixed impact parameter is given by [4,10]

$$\frac{\mathrm{d}N^{AA\to h}}{\mathrm{d}y}(y,b) = n_A(b)\left[N^{qq^{\mathrm{P}}-q_{\mathrm{v}}^{\mathrm{T}}}_{h,\mu(b)}(y) + N^{q_{\mathrm{v}}^{P}-qq^{T}}_{h,\mu(b)}(y) + (2k-2)\ N^{q_s-\overline{q}_s}_{h,\mu(b)}(y)\right] + (n(b)-n_A(b))\,2k\ N^{q_s-\overline{q}_s}_{h,\mu(b)}(y)\ . \quad (1)$$

Here

$$n(b) = \sigma_{pp}A^2\int \mathrm{d}^2s\ T_A(s)\ T_B(b-s)/\sigma_{AA}(b)\ , \quad (2)$$

where $T_A(b)$ denotes the nuclear profile function and σ_{pp} (σ_{AA}) is the pp (AA) cross-section. $n(b)$ is the average number of binary collisions and

$$n_A(b) = A\int \mathrm{d}^2s\ T_A(s)\,[1-\exp(-\sigma_{pp}\ A\ T_A(b-s)] /\sigma_{AA}(b)\ , \quad (3)$$

is the average number of participant pairs at fixed impact parameter b. P and T denote projectile and target nuclei. k is the average number of inelastic collisions in pp and $\mu(b) = k\nu(b)$ with $\nu(b) = n(b)/n_A(b)$ is the average total number of collisions suffered by each nucleon. At $\sqrt{s} = 130\,\mathrm{GeV}$ we have $k = 2$ [10].

The $N_{h,\mu(b)}(y)$ in (1) are the rapidity distributions of hadron h in each individual string. The superscript $qq^{\mathrm{P}} - q_{\mathrm{v}}^{\mathrm{T}}$ denotes a string stretched between a diquark of the projectile and a valence quark of the target while $q_{\mathrm{s}}-\overline{q}_{\mathrm{s}}$ represents a string stretched between a sea quark of the projectile and an antiquark from the target, or vice versa (in this case the string center of mass coincides with the overall center of mass). In DPM multiparticle production is the result of a color exchange. In a single inelastic collision, the nucleon splits into a valence quark and the rest of the proton (called diquark for short), and two strings

[a] Unité Mixte de Recherche UMR no. 8627 – CNRS

$qq^{\rm P}-q_{\rm v}^{\rm T}$ and $q_{\rm v}^{\rm P}-qq^{\rm T}$ are produced. Due to unitarity, multiple inelastic collisions are present in NN. In each extra collision two strings of type $q_{\rm s}-\overline{q}_{\rm s}$ are produced. In this way we obtain the expression in brackets in (1). Note that the total number of strings in each NN collision is $2k$, i.e. two strings per inelastic collision. (Actually, the number of inelastic collisions is distributed. However, this distribution is rather narrow at fixed impact parameter and no significant numerical difference has been observed by taking the average value, as in (1).) In an AA collision we have $n_A(b)$ NN collisions. Hence the factor $n_A(b)$. Moreover, each nucleon of the projectile (target) can interact with several nucleons of the target (projectile). Since the total number of binary collisions is $kn(b)$, the total number of strings in DPM is $2kn(b)$. Since all valence quarks and diquarks have been taken care of in the first lines of (1), all extra strings are of type $q_{\rm s}-\overline{q}_{\rm s}$. This explains the last line in (1). The rapidity distribution of each string is obtained from a convolution of momentum distribution and fragmentation functions[1] which are universal – i.e. the same in all hadronic and nuclear reactions.

It was shown in [10] that (1), supplemented with shadowing corrections, leads to values of charged multiplicities at mid-rapidities as a function of centrality in agreement with the data, both at SPS and RHIC. Here we use the same shadowing corrections as in [10] – leading to the lower edge of the shaded area in Fig. 4 of [10].

3 Net baryon production

For baryon production, the formalism of Sect. 2 allows one only to compute $B\overline{B}$ pair production for the different baryon species. Let us now consider the net baryon production $\Delta B = B-\overline{B}$. In the standard version of DPM [4] (or QGSM [12]) the leading baryon results from the fragmentation of a valence diquark. This component will be called diquark preserving (DP). The stopping observed in Pb–Pb collisions at SPS has led to the introduction of a new mechanism based on the transfer in rapidity of the baryon junction [5–9]. Here we follow the formalism in [3] which describes the SPS data. In an AA collision, this component, called diquark-breaking (DB), gives the following rapidity distribution of the two net baryons in a single NN collision of AA [3]

$$\left(\frac{{\rm d}N_{DB}^{\Delta B}}{{\rm d}y}(y)\right)_{\nu(b)} \qquad (4)$$
$$= C_{\nu(b)}\left[Z_+^{1/2}(1-Z_+)^{\nu(b)-3/2}+Z_-^{1/2}(1-Z_-)^{\nu(b)-3/2}\right] ,$$

where $Z_\pm=\exp(\pm y-y_{\max})$ and $\nu(b)=n(b)/n_A(b)$. $C_{\nu(b)}$ is determined from the normalization to two at each b.

[1] For pions, we use the fragmentation functions given in [10]. For simplicity, the same form is used for kaons. For $p\overline{p}$ pair production we take [11] $xD_{qq}^{p}(x)=xD_{qq}^{\overline{p}}(x)\sim(1-x)^5$ and $xD_{q}^{p}(x)=xD_{q}^{\overline{p}}(x)\sim(1-x)^3$. For the other baryon species an extra $\alpha_\rho(0)-\alpha_\phi(0)=1/2$ is added to the power of $(1-x)$ for each strange quark in the baryon [11]

The net baryon rapidity distribution in AA collisions is then given by

$$\frac{{\rm d}N^{AA\to\Delta B}}{{\rm d}y}(y,b)=n_A(b)\left[\frac{1}{\nu(b)}\left(\frac{{\rm d}N_{DP}^{\Delta B}}{{\rm d}y}(y)\right)_{\nu(b)}\right.$$
$$\left.+\ \frac{\nu(b)-1}{\nu(b)}\left(\frac{{\rm d}N_{DB}^{\Delta B}}{{\rm d}y}(y)\right)_{\nu(b)}\right] . \quad (5)$$

The physical content of (5) is as follows. Each nucleon interacts on average with $\nu(b)$ nucleons of the other nucleus. It has been argued in [3] that in only one of these collisions the string junction, carrying the baryon number, follows a valence diquark, which fragments according to the DP mechanism. In the $\nu(b)-1$ other ones, the string junction is freed from the valence diquark and net baryon production takes place according to the DB mechanism, (4). In order to conserve baryon number, we have to divide by $\nu(b)$ and multiply by the number of participating nucleons. We obtain in this way (5)[2]. This equation gives the total net baryon density[3].

In order to get the relative densities of each baryon and antibaryon species we use simple quark counting rules [3]. Denoting the strangeness suppression factor by S/L (with $2L+S=1$), baryons produced out of three sea quarks (which is the case for pair production) are given the relative weights

$$I_3=4L^3:4L^3:12L^2S:3LS^2:3LS^2:S^3 .$$

for p, n, $\Lambda+\Sigma$, Ξ^0, Ξ^- and Ω, respectively. The various coefficients of I_3 are obtained from the power expansion of $(2L+S)^3$. In the calculations we use $S=0.1$ ($S/L=0.22$). In order to take into account the decay of $\Sigma^*(1385)$ into $\Lambda\pi$, we redefine the relative rate of the Λ and Σ using the empirical rule $\Lambda=0.6\ (\Sigma^++\Sigma^-)$ – keeping, of course, the total yield of Λ plus Σ unchanged. In this way the normalization constants of all baryon species in pair production are determined from one of them. This constant, together with the relative normalization of K and π, are determined from the data for very peripheral collisions.

For net baryon production two possibilities have been considered. The first one is that the behavior in $Z^{1/2}$, (4), is associated to the transfer of the string junction without valence quarks [5,7,9]. In this case the net baryon is made out of three sea quarks and the relevant weights are given by I_3. In the second one, (4) is a pre-asymptotic term associated to the transfer of the baryon junction plus one valence quark [6,8]. In this case the relevant weights are given by I_2, i.e. from the various terms in the expansion of $(2L+S)^2$. This second possibility is favored by the

[2] In the numerical calculations we neglect the first term of (5) since the DP component gives a very small contribution at $y^*\sim 0$ at RHIC energies – about 5% of the DB one for the most central bin where its relative contribution is maximal

[3] In order to conserve strangeness locally, we have added n extra kaons to each net baryon, where n is the number of strange quarks in the produced baryon

data and will be used in the calculations presented below[4]. Since the normalization of the total net baryon yield is determined from baryon number conservation, there is no extra free normalization constant. Moreover, the total net baryon yield is not affected by final state interactions.

4 Final state interaction

The hadronic densities obtained above will be used as initial conditions in the gain and loss differential equations which govern the final state interaction. In the conventional derivation [14] of these equations, one uses cylindrical space-time variables and assumes boost invariance. Furthermore, one assumes that the dilution in time of the densities is only due to longitudinal motion, which leads to a τ^{-1}-dependence on the longitudinal proper time τ. These equations can be written as [14,3]

$$\tau \frac{\mathrm{d}\rho_i}{\mathrm{d}\tau} = \sum_{k\ell} \sigma_{k\ell}\ \rho_k\ \rho_\ell - \sum_k \sigma_{ik}\ \rho_i\ \rho_k\ . \qquad (6)$$

The first term in the r.h.s. of (6) describes the production (gain) of particles of type i resulting from the interaction of particles k and ℓ. The second term describes the loss of particles of type i due to its interaction with particles of type k. In (6) $\rho_i = \mathrm{d}N_i/\mathrm{d}y\mathrm{d}^2s(y,b)$ are the particles yields per unit rapidity and per unit of transverse area, at fixed impact parameter. They can be obtained from the rapidity densities (1) and (5) using the geometry, i.e. the s-dependence of n_A and n see (2) and (3). The procedure is explained in detail in [15]. $\sigma_{k\ell}$ are the corresponding cross-sections averaged over the momentum distribution of the colliding particles.

Equations (6) have to be integrated from initial time τ_0 to freeze-out time τ_f. They are invariant under the change $\tau \to c\tau$ and, thus, the result depends only on the ratio τ_f/τ_0. We use the inverse proportionality between proper time and densities and put $\tau_\mathrm{f}/\tau_0 = (\mathrm{d}N/\mathrm{d}y\mathrm{d}^2s(y,b))/\rho_\mathrm{f}$. Here the numerator is given by the DPM particles densities. We take $\rho_f = [3/\pi R_p^2](\mathrm{d}N^-/\mathrm{d}y)_{y^*\sim 0} = 2\,\mathrm{fm}^{-2}$, which corresponds to the charged density per unit rapidity in a pp collision at $\sqrt{s} = 130\,\mathrm{GeV}$. This density is about 70% larger [10] than at SPS energies. Since the corresponding increase in the AA density is comparable, the average duration time of the interaction will be approximately the same at CERN-SPS and RHIC – about 5 to 7 fm.

Next, we specify the channels that have been taken into account in our calculations. They are

$$\pi N \rightleftharpoons K\Lambda(\Sigma)\ , \quad \pi\Lambda(\Sigma) \rightleftharpoons K\Xi\ , \quad \pi\Xi \rightleftharpoons K\Omega. \qquad (7)$$

We have also taken into account the strangeness exchange reactions

$$\pi\Lambda(\Sigma) \rightleftharpoons KN\ , \quad \pi\Xi \rightleftharpoons K\Lambda(\Sigma)\ , \quad \pi\Omega \rightleftharpoons K\Xi\ . \qquad (8)$$

as well as the channels corresponding to (7) and (8) for antiparticles[5]. We have taken $\sigma_{ik} = \sigma = 0.2\,\mathrm{mb}$, i.e. a single value for all reactions in (7) and (8) – the same value used in [3] to describe the CERN-SPS data.

The above formalism neglects transverse expansion. This expansion seems to be rather moderate, as indicated by the fact that the HBT radii are similar at CERN-SPS and at RHIC energies. Moreover, they are of the order of the nuclear radius. In view of that, the effect induced by transverse expansion is presumably similar to the one resulting from a relative small change of the final state interaction cross-section σ.

5 Numerical results

All our results refer to mid-rapidities. The calculations have been performed in the interval $-0.35 < y^* < 0.35$. In Fig. 1a–d we show the rapidity densities of B, $\overline{B}$ and $B - \overline{B}$ [6] versus $h^- = \mathrm{d}N_{h^-}/\mathrm{d}\eta = (1/1.17)\mathrm{d}N/\mathrm{d}y$ and compare them with available data [17–19]. We see that, in first approximation, p, $\overline{p}$, Λ and $\overline{\Lambda}$ scale with h^-. Quantitatively, there is a slight decrease with centrality of p/h^- and $\overline{p}/h^-$ ratios, a slight increase of Ξ $(\overline{\Xi})/h^-$ and a larger increase of Ω $(\overline{\Omega})/h^-$. In Fig. 2a,b we plot the yields of B and $\overline{B}$ per participant, normalized to the same ratio for peripheral collisions, versus n_part. The enhancement of B and $\overline{B}$ increases with the number of strange quarks in the baryon. This increase is comparable to the one found at SPS between pA and central Pb–Pb collisions – somewhat larger for antibaryons. The ratio K^-/π^- increases by 30% in the same centrality range, between 0.11 and 0.14 in agreement with present data [20]. The ratios $\overline{B}/B$ have a mild decrease with centrality of about 15% for all baryon species – which is also seen in the data [21]. Our values for $N^{ch}/N^{ch}_\mathrm{max} = 1/2$ are $\overline{p}/p = 0.69$, $\overline{\Lambda}/\Lambda = 0.72$, $\overline{\Xi}/\Xi = 0.79$, $\Omega/\overline{\Omega} = 0.83$ [7], to be compared with the

[4] Note, however, that a non-zero value of net omegas has been observed in hA collisions [13]. This requires a non-vanishing contribution proportional to I_3. However, its effect in AA collisions is presumably small since, in this case, the net omegas are almost entirely due to final state interaction (see Sect. 5)

[5] To be precise, of all possible charge combinations in the reactions of (7), we have only kept those involving the annihilation of a light q–$\overline{q}$ pair and production of an s–$\overline{s}$ in the s-channel. The other reactions, involving three quarks in the t-channel intermediate state, have substantially smaller cross-sections and have been neglected. All channels involving π^0 have been taken with cross-section $\sigma/2$ since only one of the $u\overline{u}$ and $d\overline{d}$ components of π^0 can participate in a given charge combination. For details see the second paper of [3]

[6] A Monte Carlo calculation in a similar framework with string fusion can be found in [16]. A net proton rapidity density of about 10 for central Au Au collisions at mid-rapidities at RHIC was first predicted in [8] using a stopping mechanism similar to the one considered here

[7] In [3], the relative weights of net baryons were given by the factors $0.5(I_2 + I_3)$ – instead of I_2 used here (see Sect. 3). In this case, the values of the ratios are $\overline{p}/p = 0.70$, $\overline{\Lambda}/\Lambda = 0.71$, $\overline{\Xi}/\Xi = 0.76$ and $\overline{\Omega}/\Omega = 0.78$. Their increase with the number of strange quarks in the baryon is smaller

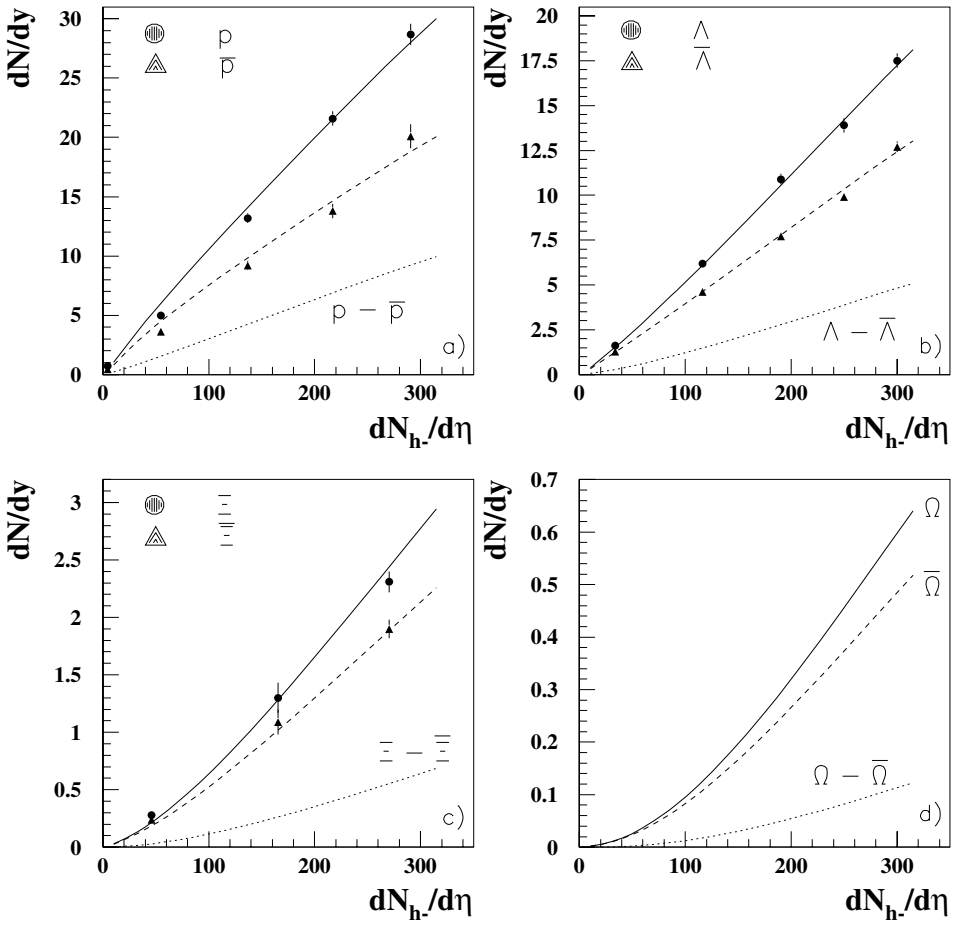

Fig. 1. a Calculated values of rapidity densities of p (solid line), $\overline{p}$ (dashed line), and $p-\overline{p}$ (dotted line) at mid-rapidities, $|y^*| < 0.35$, are plotted as a function of $\mathrm{d}N_{h^-}/\mathrm{d}\eta$, and compared with PHENIX data [17]; **b** same for Λ and $\overline{\Lambda}$ compared with preliminary STAR data [18]; **c** same for Ξ^- and $\overline{\Xi}^+$ compared to preliminary STAR data [19]; **d** same for Ω and $\overline{\Omega}$

measured values [21]

$$\overline{p}/p = 0.63 \pm 0.02 \pm 0.06\ , \quad \overline{\Lambda}/\Lambda = 0.73 \pm 0.03\ ,$$
$$\overline{\Xi}/\Xi = 0.83 \pm 0.03 \pm 0.05\ .$$

The ratio $K^+/K^- = 1.1$ and has a mild increase with centrality, a feature also seen in the data.

As explained above only one parameter has been adjusted in order to determine the absolute yields of baryons and antibaryons. This parameter controls the yield of pair produced $B\overline{B}$. Since its value has been determined from data not corrected for feed-down from week decays, our results for pair produced baryons should also be compared with non-corrected data – which is the case for both the PHENIX [17] and the STAR [18,19] data in Fig. 1. This free parameter has to be re-determined after these corrections are known. It will then be possible to compare its value with the one obtained from other sets of data, in particular pp. Likewise, the corrected yields of net protons will determine the exact amount of stopping and should allow one to decide whether or not there is "anomalous" stopping in AA, i.e. an excess as compared to an extrapolation from pp and pA. At present there is no clear indication of anomalous stopping [22].

After completion of this work, the PHENIX collaboration [23] has published the yields of p and $\overline{p}$ for the 5% most central events corrected for feed-down. The corrections are 30%. The systematic error is 20%.

6 Physical interpretation and conclusions

Before final state interactions, all ratios K/h^-, B/h^- and $\overline{B}/h^-$ decrease slightly with increasing centrality. This effect is rather marginal at RHIC energies and mid-rapidities.

The final state interactions (7) and (8) lead to a gain of strange particle yields. The reason for this is the following. In the first direct reaction of (7) we have $\rho_\pi > \rho_K$, $\rho_N > \rho_\Lambda$, $\rho_\pi \rho_N \gg \rho_K \rho_\Lambda$. The same is true for all direct reactions of (7). In view of that, the effect of the inverse reactions of (7) is small. On the contrary, in all reactions of (8), the product of the densities in the initial and final states are comparable and the direct and inverse reactions tend to compensate for each other. Baryons with the largest strange quark content, which find themselves at the end of the chain of direct reactions (7) and have the smallest yield before final state interaction, have the largest enhancement. Moreover, the gain in the yield of strange baryons is larger than the one of antibaryons since $\rho_B > \rho_{\overline{B}}$. Furthermore, the enhancement of all baryon species increases with centrality, since the gain, resulting

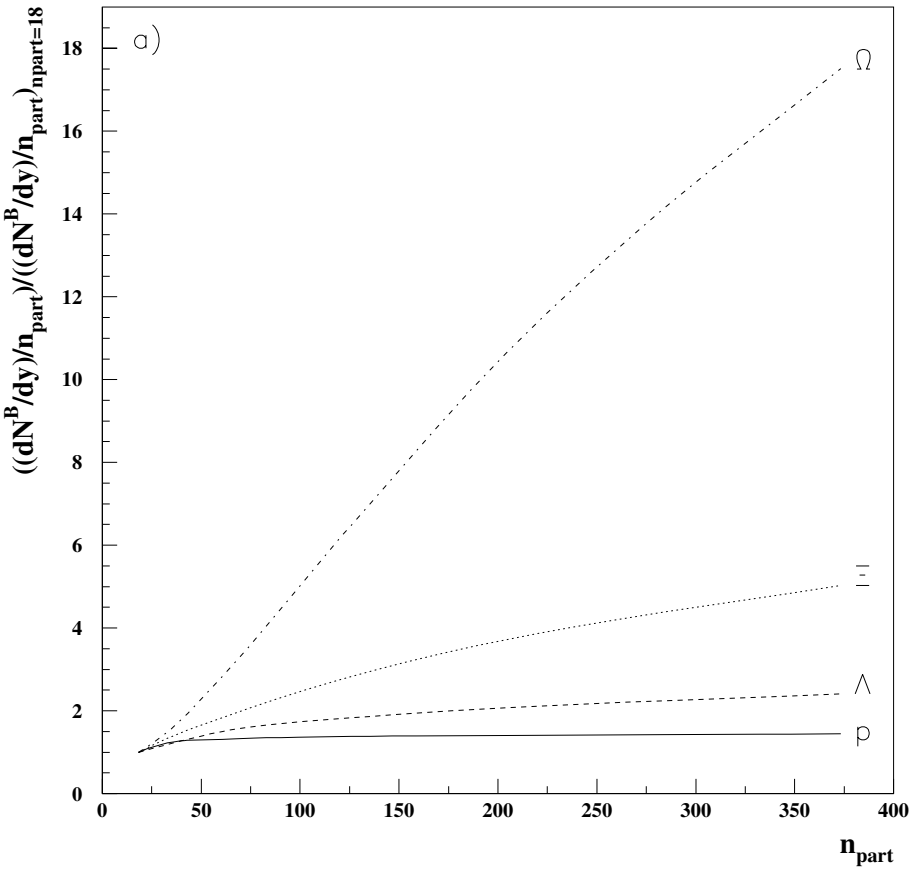

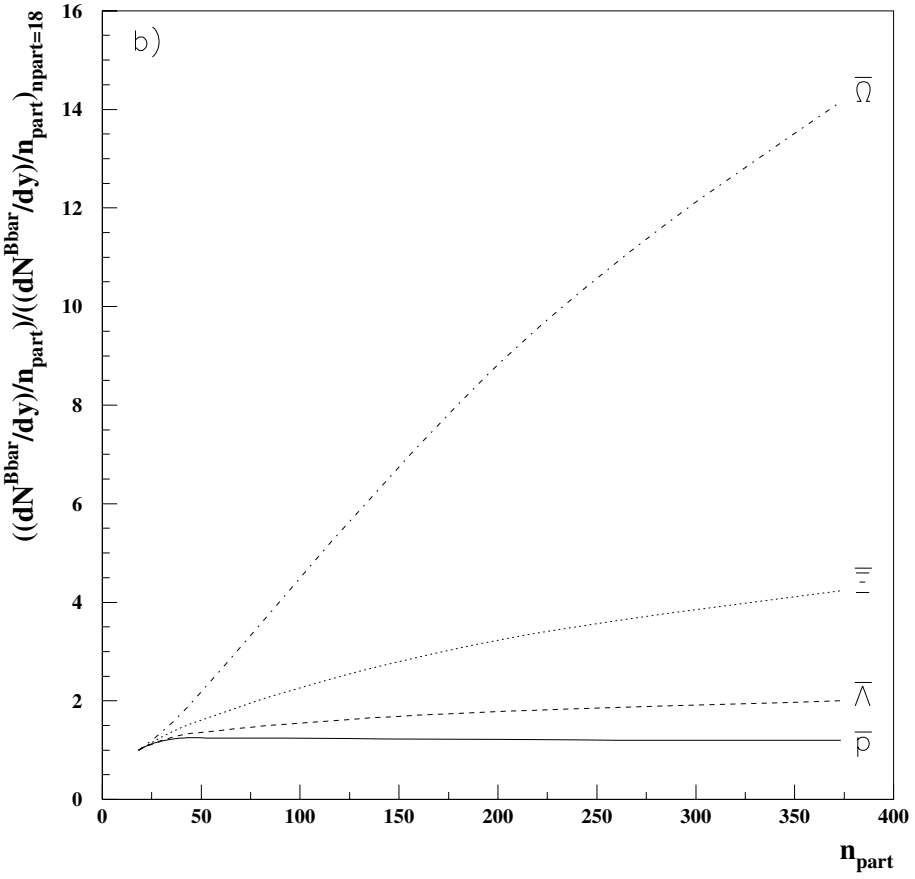

Fig. 2. Calculated values of the ratios $B/n_{\rm part}$ **a** and $\overline{B}/n_{\rm part}$ **b**, normalized to the same ratio for peripheral collisions ($n_{\rm part} = 18$), are plotted as a function of $n_{\rm part}$

from the first term in (6), contains a product of densities and thus increases quadratically with increasing centrality.

Although the inverse slopes ("temperature") have not been discussed here, let us note that in DPM they are approximately the same [24] for all baryons and antibaryons both before and after final state interaction – the effect of final state interactions being rather small [16].

We would like to emphasize the fact that in DPM (before final state interaction) the rapidity density of charged particle per participant increases with centrality. This increase is larger for low centralities [10]. This has an important effect on both the size and the pattern of strangeness enhancement in our results. It explains why the departure from a linear increase of the Ξ and Ω (concave shape) seen in Fig. 1c,d is also more pronounced for lower centralities. It leads to the convexity in the centrality dependence of the yields of hyperons and antihyperons per participant in Fig. 2 (note, however, a change of curvature for very peripheral collisions where the effect of final state interactions is negligible). This centrality pattern is a distinctive feature as well as a firm prediction of our approach.

In conclusion, we have shown that the enhancement of kaon, baryon and antibaryon production in heavy ion collisions observed at CERN-SPS and RHIC can be explained in the framework of DPM supplemented with final state interaction (comovers). The latter depend on a single adjustable parameter, the comovers interaction cross-section $\sigma_{\rm co} = 0.2\,{\rm mb}$ – the same at the two energies.

Acknowledgements. It is a pleasure to thank N. Armesto, A. Kaidalov, K. Redlich and Yu. Shabelski for discussions and C. Roy (STAR) and M.J. Tannenbaum (PHENIX) for information on the data. C.A.S. is supported by a Marie Curie Fellowship of the European Community program TMR (Training and Mobility of Researchers), under the contract number HPMF-CT-2000-01025.

References

1. WA97 coll., E.A. Andersen et al., Phys. Lett. B **433**, 209 (1998); Phys. Lett. B **449**, 401 (1999); NA57 coll., N. Carrer et al., Nucl. Phys. A **698**, 118c (2002)
2. NA49 coll., H. Appelshäuser et al., Phys. Lett. B **433**, 523 (1998); Phys. Lett. B **444**, 523 (1998); Eur. Phys. J. C **2**, 661 (1998)
3. A. Capella, C.A. Salgado, New J. Phys. **2**, 1 (2000); Phys. Rev. C **60**, 054906 (1999); A. Capella, E.G. Ferreiro, C.A. Salgado, Phys. Lett. B **459**, 27 (1999); Nucl. Phys. A **661**, 502 (1999)
4. A. Capella, U. Sukhatme, C.-I. Tan, J. Tran Thanh Van, Phys. Lett. B **81**, 68 (1979); Phys. Rep. **236**, 225 (1994)
5. G.C. Rossi, G. Veneziano, Nucl. Phys. B **123**, 507 (1977)
6. B.Z. Kopeliovich, B.G. Zakharov, Sov. J. Nucl. Phys. **48**, 136 (1988); Z. Phys. C **43**, 241 (1989)
7. D. Kharzeev, Phys. Lett. B **378**, 238 (1996)
8. A. Capella, B.Z. Kopeliovich, Phys. Lett. B **381**, 325 (1996)
9. S.E. Vance, M. Gyulassy, Phys. Rev. Lett. **83**, 1735 (1999)
10. A. Capella, D. Sousa, Phys. Lett. B **511**, 185 (2001)
11. G.H. Arakelyan, A. Capella, A. Kaidalov, Yu.M. Shabelski, Eur. Phys. J. C **26**, 81 (2002)
12. A.B. Kaidalov, Phys. Lett. B **116**, 459 (1982)
13. E769 coll., E.M. Aitala et al., Phys. Lett. B **496**, 9 (2000)
14. B. Koch, U. Heinz, J. Pitsut, Phys. Lett. B **243**, 149 (1990)
15. A. Capella, A.B. Kaidalov, D. Sousa, Phys. Rev. C **65**, 054908 (2002)
16. N.S. Amelin, N. Armesto, C. Pajares, D. Sousa, Eur. Phys. J. C **22**, 149 (2001)
17. PHENIX coll., K. Adcox et al., nucl-ex/0112006
18. STAR coll., C. Adler et al., Phys. Rev. Lett. **87**, 262302 (2001)
19. STAR coll., J. Castillo in Proceedings Quark Matter 2002, Nantes (France), to be published
20. STAR coll., H. Caines, Nucl. Phys. A **698**, 112c (2002)
21. STAR coll., C. Adler et al., Phys. Rev. Lett. **86**, 4778 (2001)
22. A. Capella, Phys. Lett. B **542**, 65 (2002)
23. PHENIX coll., K. Adcox et al., nucl-ex/0204007
24. J. Ranft, A. Capella, J. Tran Thanh Van, Phys. Lett. B **320**, 346 (1994)